

## Microwave-Enabled Synthesis of Dihydropyrazolo[4',3':5,6]pyrano[2,3-d]pyrimidine Derivatives Utilizing Hf based UiO-66 Magnetic–Metal Organic Frameworks (MMOFs)

S. P. Gawali<sup>1,2\*</sup>, S.S. Kamble<sup>1</sup>, D.V. Mane<sup>3,4</sup>

<sup>1</sup>Department of Chemistry, Sundarrao More Arts, Commerce and Science College, Poladpur, Raigad, 402303 India

<sup>2</sup>School of Science, Yashwantrao Chavan Maharashtra open University, Nashik, Maharashtra 402222 India

<sup>3</sup>Former. Regional Director, YCMOU Nashik 402222 India, <sup>4</sup>Department of Chemistry, Shri Chhatrapati Shivaji College Omerga, Dharashiv 413606 India, E-mail id- spgawali1986@gmail.com

DOI : <https://doi.org/10.5281/zenodo.18247025>

### ARTICLE DETAILS

Research Paper

Accepted: 26-12-2025

Published: 10-01-2026

### Keywords:

*Dihydropyrazolo pyrano pyrimidines, Magnetic Metal–Organic Frameworks, UiO-66(Hf), Microwaves Assited synthesis, Environmentally Friendly Chemistry.*

### ABSTRACT

An efficient, green synthetic protocol for dihydropyrazolo[4',3':5,6]pyrano[2,3-d]pyrimidine derivatives was developed using microwave irradiation and a magnetic–metal organic framework (MMOF) catalyst, Fe<sub>3</sub>O<sub>4</sub>@SiO<sub>2</sub>@UiO-66(Hf). The catalyst, synthesized via a stepwise approach, combines Fe<sub>3</sub>O<sub>4</sub>'s magnetic properties with the robust UiO-66 (Hf) framework, enabling facile separation and reuse. Characterization techniques including X-ray diffraction (XRD), Fourier-transform infrared spectroscopy (FT-IR), scanning electron microscopy (SEM), and EDX analysis confirmed the MMOF fabrication. Product compounds were identified through spectral analysis of dihydropyrazolo[4',3':5,6]pyrano[2,3-d]pyrimidine derivatives using <sup>1</sup>H NMR, <sup>13</sup>C NMR, and IR spectroscopy. The catalytic system showed high efficiency under microwave irradiation, yielding excellent results (85–94%) within short reaction times (6 min) under solvent-free conditions. Optimization studies determined optimal catalyst loading and microwave power for

maximum conversion. The catalyst showed remarkable recyclability, maintaining activity over five cycles with minimal loss. Comparative studies demonstrated superior performance over conventional catalysts in reaction rate and environmental sustainability. Mechanistic investigations suggest substrate activation via Lewis acidic Hf sites and microwave-induced heating, promoting rapid cyclization. This heterogeneous catalytic approach aligns with green chemistry principles, offering an efficient, recyclable route to valuable heterocyclic scaffolds with potential medicinal applications.

## 1. Introduction

Dihydropyrimidine-based heterocycles are an important category of nitrogen-containing compounds known for their wide range of biological activities, such as antiviral [1], anticancer [2, 4], and anti-inflammatory effects [3]. Notably, fused heterocyclic systems like dihydropyrazolo[4',3':5,6]pyrano[2,3-d]pyrimidines have garnered significant interest due to their intricate structures and potential as pharmacophores [4]. Conventional synthesis methods for these compounds typically involve multiple steps, harsh conditions, and homogeneous catalysis, which hinder their sustainability and scalability [5,6]. To overcome these issues, the development of green and heterogeneous catalytic systems has become a crucial approach. Heterogeneous catalysts provide benefits such as easy separation, reusability, and a lower environmental footprint [7]. Metal–organic frameworks (MOFs), known for their adjustable porosity, large surface area, and structural flexibility, have emerged as leading candidates in heterogeneous catalysis [8]. Specifically, hafnium-based MOFs (UiO-66(Hf)) are noted for their outstanding thermal and chemical stability, along with Lewis acidity, making them suitable for catalyzing various organic transformations [9].

Integrating magnetic nanoparticles ( $\text{Fe}_3\text{O}_4$ ) into metal-organic frameworks (MOFs) to create magnetic–metal organic frameworks (MMOFs) enhances the recovery of catalysts through magnetic separation, which is in line with environmentally friendly process design [10, 11]. Although there have been advancements, the use of Hf-based MMOFs in the microwave-assisted synthesis of fused heterocycles is still not well-explored. This research aims to fill this gap by developing a microwave-assisted, heterogeneous catalytic method using  $\text{Fe}_3\text{O}_4@\text{SiO}_2@\text{UiO-66(Hf)}$  MMOFs for synthesizing dihydropyrazolo[4',3':5,6]pyrano[2,3-d]pyrimidine derivatives. The method seeks to leverage the



advantages of microwave irradiation and MMOF catalysis to achieve a fast, efficient, and environmentally friendly synthesis of these important heterocycles.

## 2. Materials and Methods

### 2.1 Chemicals and Reagents

All the chemicals were of analytical grade and were utilized without any additional purification. Hafnium(IV) chloride ( $\text{HfCl}_4$ ), terephthalic acid, iron(III) chloride hexahydrate ( $\text{FeCl}_3 \cdot 6\text{H}_2\text{O}$ ), iron(II) chloride tetrahydrate ( $\text{FeCl}_2 \cdot 4\text{H}_2\text{O}$ ), sodium meta silicate ( $\text{Na}_2\text{SiO}_3$ ), ammonium hydroxide, ethyl acetoacetate, hydrazine hydrate, an aromatic aldehyde, barbituric acid, and other organic substrates were sourced from standard suppliers.

### 2.2 Synthesis of $\text{Fe}_3\text{O}_4@SiO_2@UiO-66$ (Hf) MMOFs

#### 2.2.1 Synthesis of $\text{Fe}_3\text{O}_4$

Magnetic magnetite ( $\text{Fe}_3\text{O}_4$ ) nanoparticles are synthesized via the chemical co-precipitation of ferric ( $\text{Fe}^{3+}$ ) and ferrous ( $\text{Fe}^{2+}$ ) ions. To achieve this, iron (III) chloride hexahydrate and iron(II) chloride tetrahydrate are dissolved in deionized water, ensuring a 2:1 ratio of  $\text{Fe}^{3+}$  to  $\text{Fe}^{2+}$  is maintained. Hydrochloric acid is introduced to inhibit premature hydroxide formation. Mercaptoethanol serves as a stabilizing agent, and the system is deoxygenated by introducing nitrogen at  $80^\circ\text{C}$ . The solution turns black upon the addition of ammonium hydroxide while stirring. Microwave irradiation is subsequently applied to crystallize the nanoparticles, which are then collected through centrifugation and dried to produce  $\text{Fe}_3\text{O}_4$  nanoparticles.

#### 2.2.2 Synthesis of $\text{Fe}_3\text{O}_4@SiO_2$

The  $\text{Fe}_3\text{O}_4@SiO_2$  composite was synthesized by applying microwave heating to  $\text{Fe}_3\text{O}_4$  nanoparticles in distilled water mixed with a sodium silicate solution. This process utilizes a modified Stöber method, which involves coating  $\text{Fe}_3\text{O}_4$  nanoparticles with  $SiO_2$ . Initially, the  $\text{Fe}_3\text{O}_4$  nanoparticles are dispersed in a water and ethanol mixture and then subjected to ultrasonication. The pH is raised to 11 using NaOH, followed by the addition of a sodium metasilicate solution. The pH is then adjusted to 9 with HCl to promote the formation of the  $SiO_2$  shell. After microwave irradiation and an overnight aging period, the  $\text{Fe}_3\text{O}_4@SiO_2$  nanoparticles are washed, magnetically separated, and dried.

### 2.2.3 Synthesis of Hf-UiO-66

Synthesis of Hf-UiO-66 involves a solvothermal approach using hafnium tetrachloride ( $\text{HfCl}_4$ ) and 1,4-benzenedicarboxylic acid ( $\text{H}_2\text{BDC}$ ).  $\text{HfCl}_4$  reacts with  $\text{H}_2\text{BDC}$  to form the hafnium-oxo cluster  $[\text{Hf}_6\text{O}_4(\text{OH})_4(\text{BDC})_6]$ , the framework's secondary building unit. The synthesis occurs in N,N-dimethylformamide (DMF) with hydrochloric acid (HCl) as modulator for crystal growth. The mixture is heated under microwave irradiation at  $80^\circ\text{C}$  with 700 W powers for few minute to form the MOF structure.

### 2.2.4 Synthesis of Hf-MMOF ( $\text{Fe}_3\text{O}_4@\text{SiO}_2\text{-UiO-66-Hf}$ )

The process starts by dispersing 1.0 g of  $\text{Fe}_3\text{O}_4@\text{SiO}_2$  in 45 mL of DMF, followed by 30 minutes of ultrasonication. Next, 2 mmol of  $\text{HfCl}_4$  (0.5567 g) is introduced, and the mixture is sonicated for an additional 10 minutes. Subsequently, 2 mmol of  $\text{H}_2\text{BDC}$  (0.332 g) dissolved in 10 mL of DMF, along with 0.9 mL of HCl, is added. The solution is then subjected to microwave heating at  $80^\circ\text{C}$  for 8 minutes at a power of 700 W, and the reaction is allowed to proceed for 12 hours. The resulting product is washed five times with DMF, separated using a strong external magnet, and dried at  $50^\circ\text{C}$  for 24 hours to yield the Hf-MMOF composite ( $\text{Fe}_3\text{O}_4@\text{SiO}_2\text{-UiO-66-Hf}$ ).

## 2.3 General Procedure for Synthesis of Dihydropyrazolo[4',3':5,6]pyrano[2,3-d]pyrimidine Derivatives

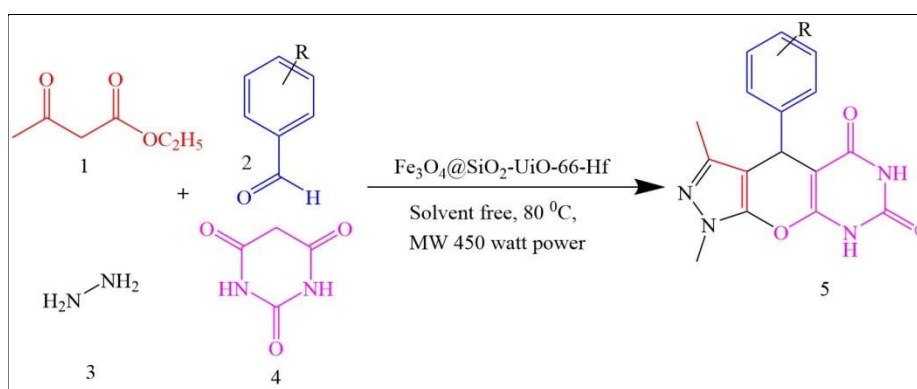


*Figure 1. Synthesis of Dihydropyrazolo[4',3':5,6]pyrano[2,3-d]pyrimidine-5,7-diones Derivatives 5 in the presence of  $\text{Fe}_3\text{O}_4@\text{SiO}_2\text{-UiO-66-Hf}$  as a catalyst*

In an environment devoid of solvents, a mixture consisting of 10 mmol each of ethyl acetoacetate, hydrazine hydrate, an aromatic aldehyde, and barbituric acid was combined with 0.1 g of the Hf-MMOF ( $\text{Fe}_3\text{O}_4@\text{SiO}_2\text{-UiO-66-Hf}$ ) catalyst. This blend was subjected to microwave irradiation at 450 W for 6

minutes, with its progress tracked using TLC. Once the reaction mixture cooled, ethanol was employed to extract the product, and the catalyst was removed through filtration. The solution was then concentrated, and pure dihydropyrazolo[4',3':5,6]pyrano[2,3-d]pyrimidine derivatives were obtained by recrystallizing from ethanol, reaction scheme see in fig.1.

### 3. Results

#### 3.1 Catalyst Characterization

##### 3.1.1 X-ray Diffraction (XRD) Analysis

Figure 2 illustrates the XRD analysis of crystalline structures, confirming the successful creation of  $\text{Fe}_3\text{O}_4$ ,  $\text{Fe}_3\text{O}_4@\text{SiO}_2$ , UiO-66, and  $\text{Fe}_3\text{O}_4@\text{SiO}_2@\text{UiO-66}$  nanoparticles. The XRD pattern for  $\text{Fe}_3\text{O}_4$ , verifies its characteristic magnetic iron oxide crystal structure [12, 13]. When  $\text{Fe}_3\text{O}_4$ , is coated with  $\text{SiO}_2$ , forming  $\text{Fe}_3\text{O}_4@\text{SiO}_2$ , the XRD peaks of  $\text{Fe}_3\text{O}_4$  remain visible, though they might appear slightly diminished or broadened due to the silica coating [13, 14]. The characterization peaks align well with the UiO-66 crystalline structure as documented in existing literature [15]. In the composite  $\text{Fe}_3\text{O}_4@\text{SiO}_2$  - UiO-66 (Hf), the XRD pattern displays features from both the  $\text{Fe}_3\text{O}_4@\text{SiO}_2$  core and the UiO-66 shell, demonstrating that the composite material retains the crystal structures of both components.

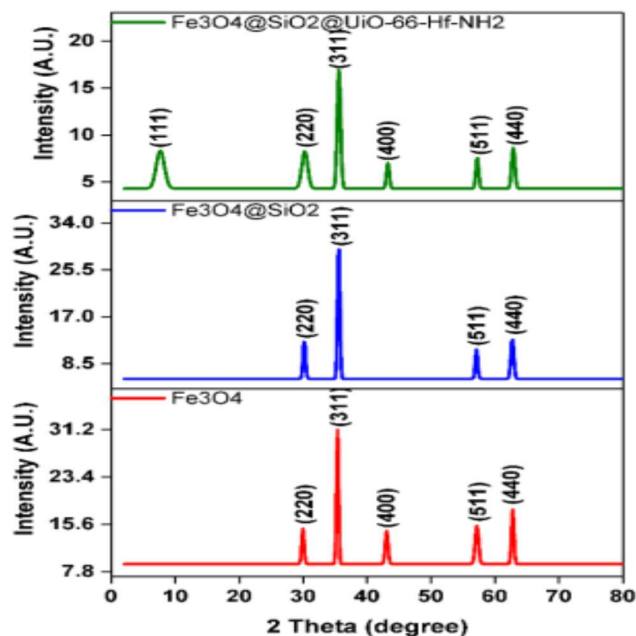


Figure 2. PXRD spectra of  $\text{Fe}_3\text{O}_4$ ,  $\text{Fe}_3\text{O}_4@\text{SiO}_2$  and  $\text{Fe}_3\text{O}_4@\text{SiO}_2$ -UiO-66 (Hf)

##### 3.1.2 Fourier Transform Infrared Spectroscopy (FTIR):

Figure 3 shows FTIR spectroscopy results of the synthesized magnetic nanoparticles. Peaks at 533 and 1028  $\text{cm}^{-1}$  confirm silica-coated magnetic nanoparticles, corresponding to Fe-O and Si-O stretching vibrations. Peaks at 1389 and 1690  $\text{cm}^{-1}$  indicate C=C and C=O bonds, confirming MPS attachment to silica-coated  $\text{Fe}_3\text{O}_4$  nanoparticles [16, 17]. The FTIR spectra showed characteristic peaks of UiO-66 and  $\text{Fe}_3\text{O}_4@UiO-66$ , including  $-\text{COO}^-$  stretching modes at 1398 and 1577  $\text{cm}^{-1}$ , carboxylic group vibrations at 1350-1700  $\text{cm}^{-1}$ , C-H bond vibrations from 2932-3100  $\text{cm}^{-1}$ , and O-H bond vibrations from 3250-3600  $\text{cm}^{-1}$  [18]. These confirm UiO-66 growth on functionalized  $\text{Fe}_3\text{O}_4$  nanoparticles.

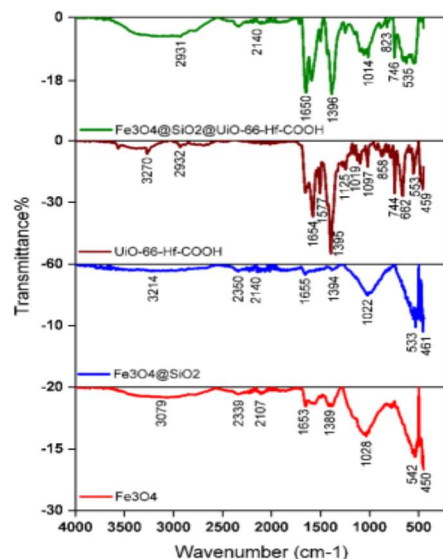


Figure 3. FTIR spectra of  $\text{Fe}_3\text{O}_4$ ,  $\text{Fe}_3\text{O}_4@SiO_2$ , UiO-66 (Hf), and  $\text{Fe}_3\text{O}_4@SiO_2\text{-UiO-66}$  (Hf)

The SEM images (fig. 4) show morphological changes across synthesis stages. SEM images showed uniform spherical particles of 150 nm. The pristine  $\text{Fe}_3\text{O}_4$  nanoparticles display uniform spherical morphology. After silica coating to form  $\text{Fe}_3\text{O}_4@SiO_2$ , particles maintain spherical shape with increased surface roughness [16, 19]. The UiO-66-Hf-based MOFs exhibit octahedral crystalline structures with faceted surfaces, where functional groups influence crystal morphology [19, 20].

EDX spectra in Fig 5. verify Fe, O, Si, and Hf elements in the samples, confirming synthesis of  $\text{Fe}_3\text{O}_4$ ,  $\text{Fe}_3\text{O}_4@SiO_2$ , UiO-66 (Hf), and  $\text{Fe}_3\text{O}_4@SiO_2\text{-UiO-66}$  (Hf).  $\text{Fe}_3\text{O}_4$  and  $\text{Fe}_3\text{O}_4@SiO_2$  show predominant Fe and O signals, with increased Si peak after silica coating [21]. The detection of Hf with other elements in UiO-66 (Hf) and  $\text{Fe}_3\text{O}_4@SiO_2\text{-UiO-66}$  (Hf) confirms metal-organic framework integration onto the magnetic core.

### 3.1.3 Scanning Electron Microscopy (SEM):

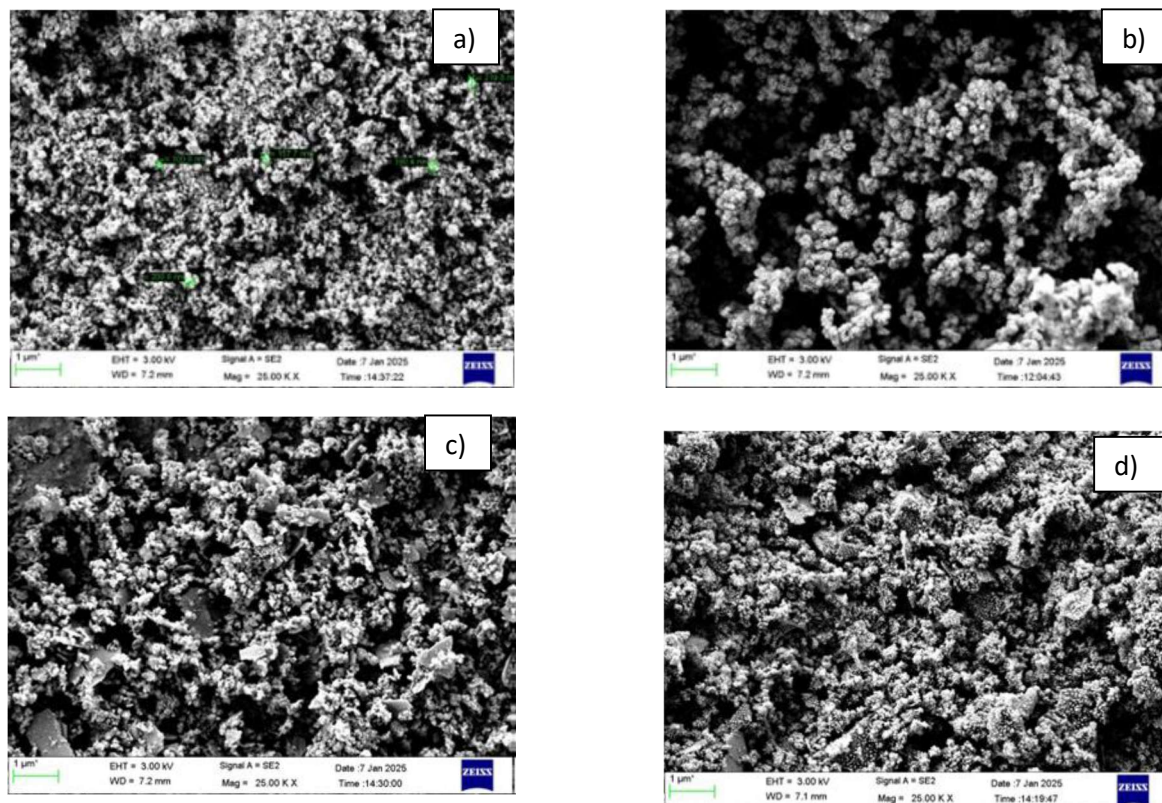


Figure 4. SEM Images of a)  $Fe_3O_4$  b)  $Fe_3O_4@SiO_2$  c)  $UiO-66 (Hf)$  d)  $Fe_3O_4@SiO_2-UiO-66 (Hf)$

### 3.1.4 Elemental Analysis (EDX)

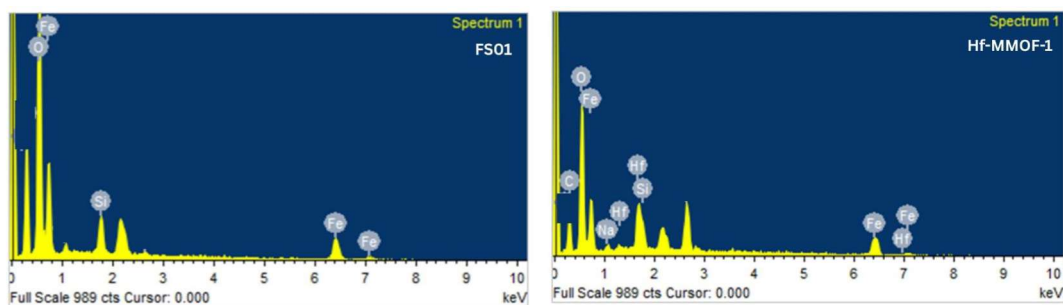


Figure 5. EDX pattern of a)  $Fe_3O_4@SiO_2$  b)  $Fe_3O_4@SiO_2-UiO-66 (Hf)$

## 3.2 Catalytic Activity and Optimization

In our preliminary research, we outline the condensation process involving ethyl acetoacetate 1, aromatic aldehydes 2, hydrazine hydrate 3, and barbituric acid 4, utilizing  $Fe_3O_4@SiO_2-UiO-66-Hf$  as a heterogeneous catalyst to synthesize Dihydropyrazolo[4',3':5,6]pyrano[2,3-d]pyrimidine Derivatives 5 (Fig. 1). Initially, we conducted experiments with ethyl acetoacetate, benzaldehyde, hydrazine hydrate,



and barbituric acid in the presence of  $\text{Fe}_3\text{O}_4@\text{SiO}_2\text{-UiO-66-Hf}$  as a catalyst, varying the catalyst amount, microwave irradiation power, and temperature to determine the optimal reaction conditions (Table 1).

Entry	Catalyst Amount (g)	Microwave Power (W)	Time (min)	Yield* (%)
1	0.00	300	10	35
2	0.05	300	10	57
3	0.10	300	10	86
4	0.15	300	10	87
5	0.20	300	10	88
6	0.10	150	10	65
7	0.10	450	10	90
8	0.10	600	10	80
9	0.10	450	4	68
10	0.10	450	6	90
11	0.10	450	8	91

\* Isolated yield. Reaction conditions ethyl acetoacetate (1 mmol), aromatic aldehydes (1 mmol), hydrazine hydrate (1 mmol), and barbituric acid (1 mmol) in the presence of  $\text{Fe}_3\text{O}_4@\text{SiO}_2\text{-UiO-66-Hf}$

Without a catalyst, the yield was restricted to 35%, highlighting the catalytic role of Hf-MMOF-1. Increasing the catalyst from 0.05 g to 0.10 g boosted the yield from 57% to 86%. Further increases in catalyst amount provided minimal benefits, indicating that 0.10 g is the optimal amount. Using 0.10 g of catalyst and a reaction time of 10 minutes, a power of 150 W resulted in a 65% yield. The yield peaked at 90% with 450 W, but decreased to 80% at 600 W, likely due to overheating. Under optimal conditions (0.10 g catalyst, 450 W), a 4-minute reaction yielded 68%, while extending the time to 6 minutes achieved a 90% yield. Longer reaction times offered little additional benefit, making 6 minutes the ideal duration. As shown in Table 1, the best result was achieved with 0.1 g of catalyst, at 450 W of microwave power for 6 minutes. After optimizing the reaction conditions, we used various aromatic aldehydes (with electron-rich or electron-deficient substituents) to synthesize other derivatives in a solvent-free environment at 80°C, 0.1 g of catalyst, and 450 W of microwave power for 6 minutes, as shown in Table 2. After the reaction, monitored by TLC, the mixture was dissolved in hot ethanol, the



heterogeneous solid catalyst was easily removed with an external permanent magnet, and after cooling the filtrate, pure crystals of the products were obtained as mentioned in Table 2.

Entry	Ar	Product	Yield (%)	M.P. °C (observed)	M.P. °C (Literature)	References
1	C <sub>6</sub> H <sub>5</sub>	5a	89.3	214-216	216-218	[22]
2	4-Cl-C <sub>6</sub> H <sub>4</sub>	5b	91.2	222-224	221-223	[22]
3	4-NO <sub>2</sub> -C <sub>6</sub> H <sub>4</sub>	5c	86.9	222-223	221-223	[23]
4	3-NO <sub>2</sub> -C <sub>6</sub> H <sub>4</sub>	5d	87.7	198-200	197-199	[23]
5	4-OCH <sub>3</sub> -C <sub>6</sub> H <sub>4</sub>	5e	87.7	190	189-190	[22]
6	2-OH-C <sub>6</sub> H <sub>4</sub>	5f	90.8	212-213	210-213	[22]
7	4-OH-C <sub>6</sub> H <sub>4</sub>	5g	85.4	256-258	254-256	[23]
8	2-Cl-C <sub>6</sub> H <sub>4</sub>	5h	86.8	152	151-152	[23]
9	2-CH <sub>3</sub> -C <sub>6</sub> H <sub>4</sub>	5i	93.6	238-240	239-241	[23]
10	4-CH <sub>3</sub> --C <sub>6</sub> H <sub>4</sub>	5j	91.0	228-230	224-227	[22]

The acid catalyst can be reactivated by stirring 24 hrs in diluted H<sub>2</sub>SO<sub>4</sub> acid solution, followed by washed with water and acetone, and dry at 150 °C in hot air oven for 24 hrs. and then reused without noticeable loss of reactivity.

### 3.3 Catalyst Recyclability

As shown in Table 3, the recovered could be Fe<sub>3</sub>O<sub>4</sub>@SiO<sub>2</sub>-UiO-66-Hf recycled for five times without any significant loss of yields.

	1 <sup>st</sup> run	2 <sup>nd</sup> run	3 <sup>rd</sup> run	4 <sup>th</sup> run	5 <sup>th</sup> run
Yield (%)	89	88	85	82	80

Recycle experiments were carried out at 1 mmole of on ethyl acetoacetate, benzaldehyde, hydrazine hydrate and barbituric acid in the presence of Fe<sub>3</sub>O<sub>4</sub>@SiO<sub>2</sub>-UiO-66-Hf at 6 min



irradiation duration.
-----------------------

Fe<sub>3</sub>O<sub>4</sub>@SiO<sub>2</sub>@UiO-66(Hf) was reused for five cycles with only a marginal decrease in yield (from 89% to 80%), indicating robust stability and reusability.

### 3.4 Structure–Activity Relationships

The combination of magnetic Fe<sub>3</sub>O<sub>4</sub> and UiO-66(Hf) provides synergistic effects: magnetic separation efficiency coupled with high surface area and Lewis acidity. The silica shell stabilizes the magnetic core and promotes MOF growth, enhancing catalyst durability. Porosity ensures substrate accessibility, critical for high catalytic turnover.

### 3.5 Green Chemistry Considerations

The solvent-free microwave-assisted protocol minimizes waste and energy consumption. Catalyst recyclability reduces material usage. The heterogeneous system avoids corrosive homogeneous acids, aligning with sustainable synthesis principles.

### 3.6 Comparative Performance

Synthesis of Dihydropyrazolo[4',3':5,6]pyrano[2,3-d]pyrimidine–5,7– diones has been reported under different conditions in the literature, as shown in Table 4. In contrast with other existing methods, the MMOF catalyst under microwave irradiation showed superior reaction rates, higher yields, and easier recovery, easy work-up, and green condition are the advantages of current methodology, highlighting its practical advantages.

Entry	Catalyst	Reaction Time	Catalyst Amount	Yield (%)	Reaction Conditions	Reference
1	DABCO	20 min	20 mol%	95	H <sub>2</sub> O, Reflux	[24]
2	Co-MOF@Ag <sub>2</sub> O nanocomposite	10 min	20 mol%	92	H <sub>2</sub> O, 50°C	[25]
3	Fe <sub>3</sub> O <sub>4</sub> /Zn-MOF magnetic	20 min	0.1 g	>85	Microwave-assisted, EtOH	[26]



4	BNPs-Caff]H <sub>2</sub> SO <sub>4</sub>	40 min	0.1 g	95	H <sub>2</sub> O, 50°C	[27]
5	TiO <sub>2</sub> nanowires	60 min	10 mol%	95	H <sub>2</sub> O, Reflux	[28]

This method outperforms many reported approaches in terms of reaction time, yield, and catalyst recovery. The use of a Hf-based MMOF catalyst is novel in this context, providing a robust platform for other heterocyclic syntheses.

#### 4. Analytical data of some selected compounds

##### 5.1 Compound 5a :3-Methyl-4-phenyl-4,8-dihydropyrazolo[4',3':5,6]pyrano[2,3-d]pyrimidine-5,7(1H,6H)-dione

Physical State : White solid

Yield: 89-95%

M.P.: 238-240 °C

<sup>1</sup>H NMR (400 MHz, DMSO-d<sub>6</sub>): δ 2.13 (s, 3H, CH<sub>3</sub>), 5.53 (s, 1H, CH), 7.09 (d, 2H, Ar), 7.22 (d, 2H, Ar), 7.25 (t, 1H, Ar), 10.220 (br s, 2H, NH), 13.25 (br s, 1H, NH) ppm

<sup>13</sup>C NMR (500 MHz, DMSO-d<sub>6</sub>): δ 165.8, 164.8, 160, 150.3, 142.0, 143.6, 127.8, 126.5, 125.4, 105.5, 91.9, 30.48, 10.12 ppm

FT-IR (KBr): 3317, 3122, 3017, 1697, 1594, 1348, 1296, 970, 773 cm<sup>-1</sup>

Mass (ESI-MS): 310.313 (100%)

##### 5.2 Compound 5b: 4-(4-Chlorophenyl)-3-methyl-4,8-dihydropyrazolo[4',3':5,6]pyrano[2,3-d]pyrimidine-5,7(1H,6H)-dione

Physical State: White solid

Yield: 91-95 %

M.P.: 222-224 °C

<sup>1</sup>H NMR (400 MHz, DMSO-d<sub>6</sub>): δ 2.32 (s, 3H, CH<sub>3</sub>), 5.60 (s, 1H, CH), 7.78 (d, 2H, Ar), 7.92 (d, 2H, Ar), 10.2 (br s, 2H, NH) ppm



$^{13}\text{C}$  NMR (500 MHz, DMSO- $d_6$ ):  $\delta$  163.1, 160.5, 160.33, 150.52, 142.9, 141.45, 130.01, 128.6, 127.6, 109.0, 91.4, 56.0, 9.9 ppm

FT-IR (KBr): 3312, 3120, 1705, 1582, 1299, 1042, 810, 732  $\text{cm}^{-1}$

Mass (ESI-MS): 330.1005 (100%)

## 5. Conclusion

A novel method using microwave-assisted, heterogeneous catalysis with  $\text{Fe}_3\text{O}_4@\text{SiO}_2@\text{UiO-66}(\text{Hf})$  MMOFs was effectively established for creating dihydropyrazolo[4',3':5,6]pyrano[2,3-d]pyrimidine derivatives. The catalyst exhibited excellent activity, selectivity, and reusability in eco-friendly, solvent-free conditions. This research offers a sustainable and efficient approach for synthesizing complex heterocycles with potential pharmaceutical applications. Future research will focus on modifying the catalyst to broaden the range of substrates and using spectroscopic techniques for mechanistic insights.

## 6. Acknowledgments

We gratefully acknowledge the support from the School of science, YCMOU University, Nashik Maharashtra from India.

## References

- Tran, T. N., & Henary, M. (2022). Synthesis and Applications of Nitrogen-Containing Heterocycles as Antiviral Agents. *Molecules*, 27(9), 2700. <https://doi.org/10.3390/molecules27092700>
- Sachdeva, H., Khatik, N., Sharma, K., Khandelwal, A. R., Saquib, M., Meena, R., & Khaturia, S. (2022). Oxygen- and Sulphur-Containing Heterocyclic Compounds as Potential Anticancer Agents. *Applied Biochemistry and Biotechnology*, 194(12), 6438–6467. <https://doi.org/10.1007/s12010-022-04099-w>
- Dinodia, M. (2023). N-heterocycles: Recent Advances in Biological Applications. *Mini-Reviews in Organic Chemistry*, 20(7), 735–747. <https://doi.org/10.2174/1570193x19666211231101747>
- Ali, T. E., Bakhotmah, D. A., & Assiri, M. A. (2020). Synthesis of some new functionalized pyrano[2,3-c]pyrazoles and pyrazolo[4',3':5,6] pyrano[2,3-d]pyrimidines bearing a chromone ring as antioxidant agents. *Synthetic Communications*, 50(21), 3314–3325. <https://doi.org/10.1080/00397911.2020.1800744>



- Zhang, J., Song, H., Cui, R., Deng, C., & Yousif, Q. A. (2020). SCMNPs@Urea/Py-CuCl<sub>2</sub>: a recyclable catalyst for the synthesis of pyrano[2,3-d]pyrimidinone and pyrano[2,3-d] pyrimidine-2,4,7-trione derivatives. *Journal of Coordination Chemistry*, 73(4), 558–578. <https://doi.org/10.1080/00958972.2020.1737681>
- Ostadzadeh, H., & Kiyani, H. (2022). Multicomponent Synthesis of Tetrahydrobenzo[b]Pyrans, Pyrano[2,3-d]Pyrimidines, and Dihydropyrano[3,2-c]Chromenes Catalyzed by Sodium Benzoate. *Polycyclic Aromatic Compounds*, 43(10), 9318–9337. <https://doi.org/10.1080/10406638.2022.2162091>
- Kohli, S., Rawat, M., Rawat, S., Saraswat, V., Rathee, G., & Nagar, S. (2024). Advancement in Heterogeneous Catalysts for the Synthesis of Benzothiazole Derivatives. *ChemistrySelect*, 9(42). <https://doi.org/10.1002/slct.202402856>
- Chen, X., Cui, Y., Liu, Y., Gong, W., Jiang, H., & Hou, B. (2017). Boosting Chemical Stability, Catalytic Activity, and Enantioselectivity of Metal-Organic Frameworks for Batch and Flow Reactions. *Journal of the American Chemical Society*, 139(38), 13476–13482. <https://doi.org/10.1021/jacs.7b06459>
- Wang, L., Liu, H., Li, S., Hou, H., Qiao, W., & Wu, J. (2023). Synergistic Effects of Lewis Acid-Base Pair Sites—Hf-MOFs with Functional Groups as Distinguished Catalysts for the Cycloaddition of Epoxides with CO<sub>2</sub>. *Inorganic Chemistry*, 62(9), 3817–3826. <https://doi.org/10.1021/acs.inorgchem.2c04078>
- Cui, H., Fu, M., Yuan, B., & Huo, J. (2017). The fabrication of magnetic metal-organic frameworks composites and their application in environment. *SCIENTIA SINICA Chimica*, 47(7), 830–843. <https://doi.org/10.1360/n032016-00199>
- Kandelous, Y. M., Nikpassand, M., & Fekri, L. Z. (2024). Recent Focuses in the Syntheses and Applications of Magnetic Metal-Organic Frameworks. *Topics in Current Chemistry (Cham)*, 382(4). <https://doi.org/10.1007/s41061-024-00475-8>
- Kumar, S., Kumar, M., & Singh, A. (2021). Synthesis and characterization of iron oxide nanoparticles (Fe<sub>2</sub>O<sub>3</sub>, Fe<sub>3</sub>O<sub>4</sub>): a brief review. *Contemporary Physics*, 62(3), 144–164. <https://doi.org/10.1080/00107514.2022.2080910>
- Camacho-Fernández, J. C., González-Quijano, G. K., Séverac, C., Dague, E., Gigoux, V., Santoyo-Salazar, J., & Martínez-Rivas, A. (2021). Nanobiomechanical behavior of Fe<sub>3</sub>O<sub>4</sub>@SiO<sub>2</sub> and Fe<sub>3</sub>O<sub>4</sub>@SiO<sub>2</sub>-NH<sub>2</sub> nanoparticles over HeLa cells interfaces. *Nanotechnology*, 32(38), 385702. <https://doi.org/10.1088/1361-6528/ac0a13>



- Sembiring, T., Kurniawan, B., Nurbillah, A., Lubis, H., Lubis, R. Y., Sitingjak, N. R. L., & Noer, Z. (2024). Synthesis and characterization of Magnetic Fe<sub>3</sub>O<sub>4</sub>/SiO<sub>2</sub> composite for Environmental Sanitation. *Journal of Physics: Conference Series*, 2733(1), 012027. <https://doi.org/10.1088/1742-6596/2733/1/012027>
- Ediati, R., Mukminin, A., Nugroho, K. A., Zulfa, L. L., Kusumawati, Y., Nadjib, M., & Sulistiono, D. O. (2019). One-pot solvothermal synthesis and characterization of UiO-66/HKUST-1 composites. *IOP Conference Series: Materials Science and Engineering*, 578(1), 012072. <https://doi.org/10.1088/1757-899x/578/1/012072>
- Petreanu, I., Niculescu, V.-C., Enache, S., Iacob, C., & Teodorescu, M. (2022). Structural Characterization of Silica and Amino-Silica Nanoparticles by Fourier Transform Infrared (FTIR) and Raman Spectroscopy. *Analytical Letters*, ahead-of-print(ahead-of-print), 390–403. <https://doi.org/10.1080/00032719.2022.2083144>
- Dawn, R., Zzaman, M., Faizal, F., Kiran, C., Kumari, A., Shahid, R., Panatarani, C., Joni, I. M., Verma, V. K., Sahoo, S. K., Amemiya, K., & Singh, V. R. (2022). Origin of Magnetization in Silica-coated Fe<sub>3</sub>O<sub>4</sub> Nanoparticles Revealed by Soft X-ray Magnetic Circular Dichroism. *Brazilian Journal of Physics*, 52(3). <https://doi.org/10.1007/s13538-022-01102-x>
- Lyu, J., Bai, P., Xiao, Z., Liu, H., Guo, X., Zhang, J., & Zeng, Z. (2017). Metal–Organic Framework UiO-66 as an Efficient Adsorbent for Boron Removal from Aqueous Solution. *Industrial & Engineering Chemistry Research*, 56(9), 2565–2572. <https://doi.org/10.1021/acs.iecr.6b04066>
- Chen, R., Liu, Z., Wang, J., Tao, C.-A., Zhang, Z., & Chen, X. (2019). Layer-by-Layer Fabrication of Core-Shell Fe<sub>3</sub>O<sub>4</sub>@UiO-66-NH<sub>2</sub> with High Catalytic Reactivity toward the Hydrolysis of Chemical Warfare Agent Simulants. *ACS Applied Materials & Interfaces*, 11(46), 43156–43165. <https://doi.org/10.1021/acsami.9b14099>
- Semivrazhkaya, O. O., Ranocchiaro, M., Sushkevich, V. L., Van Bokhoven, J. A., Salionov, D., Bjelić, S., Nachtegaal, M., Verel, R., Clark, A. H., & Casati, N. P. M. (2023). Deciphering the Mechanism of Crystallization of UiO-66 Metal-Organic Framework. *Small*, 19(52). <https://doi.org/10.1002/smll.202305771>
- Asab, G., Zereffa, E. A., & Abdo Seghne, T. (2020). Synthesis of Silica-Coated Fe<sub>3</sub>O<sub>4</sub> Nanoparticles by Microemulsion Method: Characterization and Evaluation of Antimicrobial Activity. *International Journal of Biomaterials*, 2020(3–4), 1–11. <https://doi.org/10.1155/2020/4783612>



- Bakherad, M., Gholizadeh, M., Keivanloo, A., Javanmardi, M., & Doosti, R. (2016). Using magnetized water as a solvent for a green, catalyst-free, and efficient protocol for the synthesis of pyrano[2,3-c]pyrazoles and pyrano[4',3':5,6]pyrazolo [2,3-d]pyrimidines. *Research on Chemical Intermediates*, 43(2), 1013–1029. <https://doi.org/10.1007/s11164-016-2680-y>
- Momeni, S., & Ghorbani-Vaghei, R. (2024). Copper Immobilized on Modified LDHs as a Novel Efficient Catalytic System for Three-Component Synthesis of Pyrano[2,3-d]pyrimidine and pyrazolo[4',3':5,6]pyrano[2,3-d]pyrimidine Derivatives. *ACS Omega*, 9(9), 10332–10342. <https://doi.org/10.1021/acsomega.3c07913>
- Heravi, M. M., Mousavizadeh, F., Tajbakhsh, M., & Ghobadi, N. (2014). ChemInform Abstract: A Green and Convenient Protocol for the Synthesis of Novel Pyrazolopyranopyrimidines via a One-Pot, Four-Component Reaction in Water. *ChemInform*, 45(28), no. <https://doi.org/10.1002/chin.201428171>
- Hootifard, G., Sheikhhosseini, E., Ahmadi, S. A., & Yahyazadehfar, M. (2023). Synthesis and characterization of Co-MOF@Ag<sub>2</sub>O nanocomposite and its application as a nano-organic catalyst for one-pot synthesis of pyrazolopyranopyrimidines. *Scientific Reports*, 13(1). <https://doi.org/10.1038/s41598-023-44667-6>
- Bashar, B. S., Kareem, H. A., Hasan, Y. M., Ahmad, N., Alshehri, A. M., Al-Majdi, K., Hadrawi, S. K., Al Kubaisy, M. M. R., & Qasim, M. T. (2022). Application of novel Fe<sub>3</sub>O<sub>4</sub>/Zn-metal organic framework magnetic nanostructures as an antimicrobial agent and magnetic nanocatalyst in the synthesis of heterocyclic compounds. *Frontiers in Chemistry*, 10. <https://doi.org/10.3389/fchem.2022.1014731>
- Rostami, A., Darvishi, N., Navasi, Y., Pourshiani, O., & Saadati, S. (2017). Magnetic nanoparticle-supported DABCO tribromide: a versatile nanocatalyst for the synthesis of quinazolinones and benzimidazoles and protection/deprotection of hydroxyl groups. *New Journal of Chemistry*, 41(17), 9033–9040. <https://doi.org/10.1039/c7nj00479f>
- Farooq, S., & Ngaini, Z. (2020). Chalcone Derived Pyrazole Synthesis via One-pot and Two-pot Strategies. *Current Organic Chemistry*, 24(13), 1491–1506. <https://doi.org/10.2174/1385272824999200714101420>

